

1 **Distribution of branched glycerol dialkyl glycerol tetraethers in**
2 **surface soils of Qinghai–Tibetan Plateau: implications of brGDGTs-**
3 **based proxies in cold and dry regions**

4 Su Ding¹, Yunping Xu^{1*}, Yinghui Wang¹, Yue He², Juzhi Hou², Litong Chen³, Jin-
5 Sheng He^{1,3}

6 ¹MOE Key Laboratory for Earth Surface Processes, College of Urban and
7 Environmental Sciences, Peking University, Beijing 100871, China

8 ²Key Laboratory of Tibetan Environment Changes and Land Surface Processes, Institute
9 of Tibetan Plateau Research, Chinese Academy of Sciences, Beijing 100085, China

10 ³Key Laboratory of Adaptation and Evolution of Plateau Biota, Northwest Institute of
11 Plateau Biology, Chinese Academy of Sciences, Xining 810008, China

12 *Correspondence to:* Yunping Xu (yunpingxu@pku.edu.cn)
13

14 **Abstract.** The methylation index of branched tetraethers (MBT) and cyclization ratio of
15 branched tetraethers (CBT) based on the distribution of branched glycerol dialkyl
16 glycerol tetraethers (brGDGTs) are useful proxies for the reconstruction of mean annual
17 air temperature (MAT) and soil pH. Recently, a series of 6-methyl brGDGTs were
18 identified which were previously co-eluted with 5-methyl brGDGTs. However, little is
19 known about 6-methyl brGDGTs in Qinghai-Tibet Plateau (QTP), a critical region of the
20 global climate system. Here, we analyze 30 surface soils covering a large area of QTP,
21 among which 6-methyl brGDGTs were the most abundant components (average 53 ± 17 %
22 of total brGDGTs). The fractional abundance of 6-methyl brGDGTs showed a good
23 correlation with soil pH, while the global MBT_{5ME} calibration overestimates MAT in
24 the QTP. We therefore proposed a MBT_{5/6} index including both 5- and 6-methyl
25 brGDGTs, presenting a strong correlation with MAT in QTP: $\text{MAT} = -20.14 +$
26 $39.51 \times \text{MBT}_{5/6}$ ($n = 27, r^2 = 0.82; \text{RMSE} = 1.3 \text{ } ^\circ\text{C}$). Another index, namely IBT
27 based on carbon skeleton isomerism of 5-methyl to 6-methyl brGDGTs, is dependent on
28 soil pH: $\text{pH} = 6.77 - 1.56 \times \text{IBT}$ ($n = 27; r^2 = 0.74, \text{RMSE} = 0.32$). Our study

29 suggests that changing the position of methyl group of brGDGTs may be another
30 mechanism for some soil bacteria to adapt ambient pH change besides well-known
31 cyclization.

32

33 **1. Introduction**

34 The Qinghai–Tibetan Plateau (QTP), with an area of over 2.5 million km² and an
35 average elevation of over 4000 meters above sea level (a.s.l.), is the world highest and
36 largest mountain plateau. The uplift of the QTP since early Cenozoic profoundly
37 influences regional and global climates such as the evolution of Asian monsoon which
38 affects lives of over two billion people (An et al., 2001; Li, 1991; Lin et al., 2008; Wang
39 et al., 2008). A number of studies have showed that the QTP is a highly sensitive area
40 for global climate change (e.g., Kang et al., 2010; Liu & Chen, 2000; Qiu, 2008; Yao et
41 al., 2007). The record of 97 meteorological stations located over 2000 meters a.s.l. in
42 China reveals that winter temperature rise is 0.32 °C per decade in the QTP since 1950s,
43 approximately three times the global warming rate (Liu & Chen, 2000). However, the
44 history of instrumental measurement is too short to fully record the evolution of the QTP
45 climate. The reconstruction of the QTP temperature beyond instrumental measurement
46 is challenging because few quantitative proxies are available. Microfossil assemblages
47 based on pollen, diatom or chironomid are commonly used paleothermometers, but they
48 are also influenced by precipitation, salinity, nutrient or other environmental factors (e.g.,
49 Keatley et al., 2009; Meriläinen et al., 2000; Seppä & Birks, 2001). The $\delta^{18}\text{O}$ value of
50 ice core in the QTP shows a good correlation with northern hemisphere temperature
51 (Thompson et al., 1997; Yao et al., 2002). Unfortunately, ice core with a long term,
52 continuous record is lacking in most QTP.

53 Over the past decades, two molecular proxies have been developed for estimation
54 of continental temperature. The first one, namely UK'37, is based on the distribution of
55 haptophyte-derived long-chain alkenones. This proxy was originally proposed for
56 paleoceanography (Brassell et al., 1986; Prahl et al., 1988), but was found applicable for
57 reconstruction of lake surface temperature (e.g., Liu et al., 2006; Zink et al., 2001). A
58 major limitation of UK'37 is that long-chain alkenones are not always present in lakes,

59 although they were reported in some QTP lakes (e.g., Chu et al., 2005; Liu et al., 2011;
 60 Liu et al., 2006). In addition, salinity influences the compositions of long-chain
 61 alkenones in lakes (Liu et al., 2011). Besides UK'37, the methylation index of branched
 62 tetraethers (MBT) and cyclization ratio of branched tetraethers (CBT) can be also used
 63 to infer past continental temperature based on the distribution of branched glycerol
 64 dialkyl glycerol tetraethers (brGDGTs) (Weijers et al., 2007b):

$$65 \quad \text{MBT} = \frac{\text{Ia}+\text{Ib}+\text{Ic}}{\text{Ia}+\text{Ib}+\text{Ic}+\text{IIa}+\text{IIb}+\text{IIc}+\text{IIIa}+\text{IIIb}+\text{IIIc}+\text{IIa}'+\text{IIb}'+\text{IIc}'+\text{IIIa}'+\text{IIIb}'+\text{IIIc}'} \quad (1)$$

$$66 \quad \text{CBT} = -\log \frac{\text{Ib}+\text{IIb}+\text{IIb}'}{\text{Ia}+\text{IIa}+\text{IIa}'} \quad (2)$$

67 where roman numbers denote relative abundance of compounds in Fig. 1. It should be
 68 pointed out that the Eq. 1 and 2 are rewritten from original definitions because the peaks
 69 previously identified as pure 5-methyl brGDGTs (Weijers et al., 2007b) are actually
 70 mixtures of 5-methyl and 6-methyl isomers (De Jonge et al., 2013).

71 So far, only two species of Acidobacteria were identified to produce brGDGTs
 72 (Sinninghe Damsté et al., 2011), but the ubiquitous occurrence of brGDGTs in soils/peats,
 73 lakes and marginal seas suggest that other biological sources are likely (Schouten et al.,
 74 2013 and references therein). By analyzing globally distributed soils, Weijers et al.
 75 (2007b) found that the MBT is controlled by mean annual air temperature (MAT) and to
 76 less extent by soil pH, whereas CBT only relates to soil pH. Such relationship was
 77 corroborated by the subsequent study of Peterse et al. (2012) who proposed a simplified
 78 format of MBT (or MBT') based on seven quantifiable brGDGTs.

79 Since the advent, the MBT(MBT')-CBT paleotemperature proxy has been
 80 increasingly used for lakes (e.g., D'Anjou et al., 2013; Loomis et al., 2012; Sun et al.,
 81 2011), paleosol-loess sequences (e.g., Peterse et al., 2011; Zech et al., 2012), peat
 82 (Ballantyne et al., 2010) and marginal seas (e.g., Bendle et al., 2010; Weijers et al., 2007a;
 83 Zell et al., 2014). However, a relatively large scatter in global MBT/CBT-MAT
 84 calibrations (about 5 °C for root mean square error; RMSE) suggests that other factors
 85 besides temperature may influence brGDGTs-based indices (Peterse et al., 2012; Weijers
 86 et al., 2007b). In arid and semiarid areas such as western United States where
 87 precipitation is the ecological limiting factor, mean annual precipitation (MAP) rather

88 than MAT is the most important factor that affects brGDGT compositions (Dirghangi et
 89 al., 2013; Menges et al., 2014). The updated global calibration of MBT'-CBT indices
 90 (Peterse et al., 2012) also shows a weak correlation with MAT for those soil samples
 91 from arid regions (MAP < 500 mm). Some studies suggest that regional calibrations are
 92 needed to improve accuracy of the GDGTs-based proxy (e.g., Loomis et al., 2012;
 93 Pearson et al., 2011; Shanahan et al., 2013; Zink et al., 2010).

94 Another factor to cause the relatively large scatter of the MBT/CBT-MAT
 95 calibration is analytical error. By applying advanced analytical techniques, De Jonge et
 96 al. (2013) identified a series of novel 6-methyl brGDGTs which previously co-eluted
 97 with 5-methyl GDGTs that were used to calculate the brGDGTs proxies. The successful
 98 separation of 5- and 6-methyl brGDGTs resulted in a set of new brGDGT proxies, which
 99 were used to recalibrate traditionally defined MBT-CBT indexes (De Jonge et al., 2014):

$$100 \quad \text{MBT}'_{5\text{ME}} = \frac{\text{Ia} + \text{Ib} + \text{Ic}}{\text{Ia} + \text{Ib} + \text{Ic} + \text{IIa} + \text{IIb} + \text{IIc} + \text{IIIa}} \quad (3)$$

$$101 \quad \text{MAT} = -8.57 + 31.45 \times \text{MBT}'_{5\text{ME}} \\ 102 \quad (n = 222, r^2 = 0.66; \text{RMSE} = 4.8 \text{ }^\circ\text{C}, P < 0.001) \quad (4)$$

$$103 \quad \text{CBT}_{5\text{ME}} = -\log \frac{\text{Ib} + \text{IIb}}{\text{Ia} + \text{IIa}} \quad (5)$$

$$104 \quad \text{pH} = 7.84 - 1.73 \times \text{CBT}_{5\text{ME}} \\ 105 \quad (n = 221, r^2 = 0.60; \text{RMSE} = 0.84, P < 0.001) \quad (6)$$

$$106 \quad \text{CBT}' = \log \frac{\text{Ic} + \text{IIa}' + \text{IIb}' + \text{IIc}' + \text{IIIa}' + \text{IIIb}' + \text{IIIc}'}{\text{Ia} + \text{IIa} + \text{IIIa}} \quad (7)$$

$$107 \quad \text{pH} = 7.15 + 1.59 \times \text{CBT}' \\ 108 \quad (n = 221, r^2 = 0.85; \text{RMSE} = 0.52, P < 0.001) \quad (8)$$

109 For the QTP, several studies have reported GDGTs in lakes, mountains, hot springs
 110 and paleo-soils (e.g., Günther et al., 2014; He et al., 2012; Liu et al., 2013; Wang et al.,
 111 2012; Wu et al., 2013; Xie et al., 2012). Wang et al. (2012) analyzed GDGTs in surface
 112 sediments of the Lake Qinghai and surrounding soils, showing that brGDGTs-inferred
 113 MAT and soil pH were consistent with measured values. In contrast, Wu et al. (2013)
 114 found that brGDGTs-derived MAT was higher than instrumentally measured MAT in
 115 Kusai Lake sediments from the QTP. Based on the distributions of GDGTs in surface
 116 sediments of the QTP lakes, Günther et al. (2014) developed the local calibration of

117 MBT²-CBT ($r^2 = 0.59$; RMSE = 1.2 °C). However, there are only 9 lake sediments
118 included in Günther et al. (2014). For the application of MBT-CBT indices in lakes,
119 brGDGTs in lake sediments must be exclusively derived from inputs of surrounding soils.
120 However, in-situ production of brGDGTs occurs in various lakes (e.g., Blaga et al., 2009;
121 Blaga et al., 2010; Fietz et al., 2012; Pearson et al., 2011; Sinninghe Damsté et al., 2009;
122 Tierney & Russell, 2009). Furthermore, the 6-methyl brGDGTs were not reported in any
123 QTP studies, which may explain the relatively low r^2 value of the MBT/CBT-MAT
124 calibration (e.g., Günther et al., 2014). Given these facts, a direct investigation of soils
125 with improved chromatography is needed to understand environmental influences on the
126 brGDGT distributions in the QTP.

127 Here, we analyzed all 5- and 6-methyl brGDGTs in 30 surface soils from the QTP.
128 Our main objectives are to (1) determine the relative abundance and distribution of 5-
129 and 6-methyl brGDGTs in the QTP soils; (2) evaluate the effect of recently identified 6-
130 methyl brGDGTs on soil pH in the QTP; and (3) test whether global brGDGTs-MAT
131 calibration is applicable in the QTP and thereby understand the influence of temperature,
132 precipitation and soil pH on 5- and 6-methyl brGDGTs in the QTP.

133

134 **2. Materials and methods**

135 **2.1. Sampling**

136 A total of 30 surface soil samples (0-10 cm) were collected during two fieldworks
137 in 2011 and 2012, which cover a large area of the QTP (84.64°~101.20°E; 28.24°~37.45°
138 N) (Fig. 2). Sampling sites are typical alpine meadow, alpine steppe or alpine meadow
139 steppe. The extremely dry winter results in the lack of persistent snow cover in most
140 sampling sites. The soil samples were air-dried and passed through a 2 mm mesh to
141 remove large gravels. Fine roots (if present) were picked up by steel tweezers. The
142 detailed information on the sampling sites and environmental variables are listed in the
143 supplementary material (Table S1).

144

145 **2.2 Climate data**

146 There are about 70 meteorological stations in the QTP, mainly distributed in the

147 eastern part and northern border of the QTP. Thus, direct observation data on temperature
148 and precipitation at our sampling sites are generally lacking. In this study, we use the
149 WorldClim dataset (Hijmans et al., 2005) to interpolate annual, seasonal and monthly
150 mean precipitation and temperature (Table S1). The local climate is dry and cold. The
151 MAT of our sampling sites ranges from -5.5 to 7.6 °C with a vertical lapse rate of
152 0.487 °C/100 m to 0.699 °C/100 m (Cheng et al., 2012). The vertical lapse rate of air
153 temperature decreases from north to south of the QTP. The mean annual precipitation
154 (MAP) at different altitudes varies from ca. 85 mm to ca. 495 mm. The integrated maps
155 are derived from monthly temperature and precipitation values gathered from thousands
156 of weather stations around the world from 1950 to 2000 (47,554 locations for
157 precipitation and 24,542 locations for temperature). The original point data was splines
158 interpolated using latitude and longitude at a fine resolution, making it possible to obtain
159 a reasonable estimation of climatic conditions at individual sites. The WorldClim GIS
160 data used contain annual average of 6 climate variables at a 30 arc seconds resolution
161 (~1 km resolution; <http://www.worldclim.org/current.htm>). Besides MAT and MAP,
162 additional four climate variables were also used to evaluate the relationship between
163 climate and 5- and 6-methyl brGDGTs indices, including Mean Temperature of Wettest
164 Quarter (MWQT), Mean Temperature of Driest Quarter (MDQT), Mean Temperature of
165 Warmest Quarter (MWQT'), Mean Temperature of Coldest Quarter (MCQT). A total of
166 30 sites from QTP cold and dry regions (Table S1) were extracted by 6 climate variables
167 using Arcgis 9.3.

168

169 **2.3 Soil pH and brGDGT analyses**

170 For pH measurement, soils were mixed with deionized water in a ratio of 1/2.5
171 (g/ml). The soil pH values were determined by a pH meter with a precision of ±0.01 pH.
172 The pH was reported as an average of three duplicate measurements for each sample
173 with standard deviation of ±0.05.

174 The detailed procedure for lipid extraction was described by Wu et al. (2014). About
175 6 g dry soils were mixed with 600 ng C₄₆ GDGT (internal standard) (Huguet et al., 2006)
176 and ultrasonically extracted with 20 ml dichloromethane (DCM)/methanol (3:1 v:v) for

177 15 min (3×). The combined extracts were concentrated to near dryness by a rotary
178 evaporator and transferred to small vials. The concentrated extracts were completely
179 dried under a mild stream of N₂ and re-dissolved in DCM. The total extracts were
180 separated into two fractions by 5 ml hexane/DCM (9:1 v:v) and 5 ml DCM/methanol
181 (1:1 v:v), respectively, on silica gel columns. The latter fraction containing brGDGTs
182 was dissolved in 300 µl hexane/EtOAc (84:16,v/v).

183 The GDGTs were analyzed on an Agilent 1200 High Performance Liquid
184 Chromatography-atmospheric pressure chemical ionization-triple quadruple mass
185 spectrometry (HPLC-APCI-MS²) system (Yang et al., 2015). The injection volume was
186 10 µl. The separation of 5- and 6-methyl brGDGTs was achieved with two silica columns
187 in sequence (150 mm × 2.1 mm; 1.9 µm, Thermo Finnigan; USA) at a constant flow of
188 0.2 ml per min. The solvent gradient was: 84% A (hexane) and 16% B (EtOAc) for 5
189 min, then increasing the amount of B from 16% at 5 min to 18% at 65 min, and then to
190 100% B in 21 min. The column was flushed with 100% B for 4 min, and then back to
191 84/16 A/B to equilibrate it for 30 min. The APCI and MS conditions were: vaporizer
192 pressure of 4.2×10^5 Pa, vaporizer temperature of 400 °C, drying gas flow of 6 L min⁻¹,
193 temperature of 200 °C, capillary voltage of 3500 V, and corona current of 5 µA (3.2
194 kV). Peak integration was carried out using Agilent MassHunter. Samples were
195 quantified based on comparisons of the respective protonated-ion peak areas of each
196 GDGT to the internal standard in selected ion monitoring (SIM) mode. The protonated
197 ions were m/z 1050, 1048, 1046, 1036, 1034, 1032, 1022, 1020, 1018 and 744 (C₄₆
198 GDGTs). Since we assume same response factors among different brGDGTs and C₄₆
199 GDGTs, our study can be only regarded as semi-quantification.

200

201 **2.4 Statistical analyses**

202 In order to assess the relationship of 5- and 6-methyl brGDGT distributions with
203 environmental variables such as temperature, precipitation and soil pH, we performed
204 redundancy analysis (RDA) (van den Wollenberg, 1977), a constrained form of the linear
205 ordination method of principal components analysis (PCA). Species (fractional
206 abundance of 15 brGDGTs) were centered and standardized with zero average and unit

207 variance before RDA. The significance of the explanatory variances within a 1%
208 confidence interval was tested with 999 unrestricted Monte Carlo permutations.
209 Subsequently, a series of partial RDAs (pRDA) were performed to constrain the unique
210 and independent influence of individual environmental parameter alone, as well as
211 compared to all other parameters. All statistical analyses were performed with the
212 CANOCO version 4.5 software (Wageningen UR, USA).

213

214 **3. Results and discussion**

215 **3.1 brGDGTs abundance in the QTP soils**

216 All soil samples except for P790, P840 and P855 contain detectable amounts of
217 brGDGTs. Consequently, 27 soils were used to calibrate brGDGTs' indices in this study.
218 With the application of two silica LC columns in tandem, 5-methyl and 6-methyl
219 brGDGT isomers were successfully separated, increasing the number of detectable
220 brGDGT compounds from 9 (Peterse et al., 2012; Weijers et al., 2006) to 15 (Fig. 1).
221 There were three tetra-methylated brGDGTs (Ia, Ib and Ic), six penta-methylated
222 brGDGTs (IIa, IIb, IIc, IIa', IIb', IIc') and six hexa-methylated brGDGTs (IIIa, IIIb, IIIc,
223 IIIa', IIIb', IIIc'). The mean fractional abundance of 5-methyl brGDGTs (f_{5ME}) and 6-
224 methyl brGDGTs (f_{6ME}) was shown in Fig. 3. The 6-methyl brGDGTs accounted for
225 average 53% of the total amount of brGDGTs, which were dominated by IIa' and IIIa'.
226 Such composition of brGDGTs is different from that of the global soils (239 soils) that
227 5-methyl brGDGT (Ia and IIa) are usually the most abundant isomers and 6-methyl
228 brGDGTs only comprise on average 24% of the total amounts of brGDGTs (De Jonge et
229 al., 2014), suggesting that the brGDGT-producing bacteria may change their membrane
230 lipids to adapt environmental conditions. So far, two species of Acidobacteria are only
231 identified biological sources for brGDGTs, but they only produce tetra-methylated
232 brGDGTs (Sinninghe Damsté et al., 2011). In our study, the majority of the QTP soils
233 are weak alkaline (6.2~8.4 pH unit), which may favor thriving of non-Acidobacteria and
234 thereby lead to the higher proportion of 6-methyl brGDGTs.

235

236 **3.2 Environmental control on brGDGT distributions in QTP**

237 A number of studies have demonstrated that temperature, precipitation and pH are
238 the most important factors that affect the brGDGT distributions in soils (e.g., De Jonge
239 et al., 2014; Dirghangi et al., 2013; Peterse et al., 2012; Weijers et al., 2006; Weijers et
240 al., 2007b; Yang et al., 2015; Yang et al., 2014). In order to evaluate the contribution of
241 these parameters to 5- and 6-methyl brGDGT distributions in the QTP, a RDA was
242 performed (Fig. 4). The first component explains 65.2% of the variance, mainly
243 reflecting the variation in soil pH and to less extent MAP. Soil pH presents strong
244 positive relationships with fractional abundance of brGDGTs IIIa', I Ib', I Ib, and negative
245 relationships with that of IIIa, I Ia, I Ia. The second component of the RDA plot explains
246 6.1% of total variance, mainly reflecting the variation in MAT and MAP. The brGDGT-
247 IIIa', IIIa, I Ia, I Ib, I Ic show negative relationships with MAT (in the lower part of RDA),
248 whereas brGDGT-I Ia, I Ia, I Ib and I Ic present positive relationships with MAT (in the upper
249 part of RDA). These results support a physiological mechanism that soil bacteria change
250 the number of methyl branches of brGDGTs with temperature in order to maintain
251 acceptable fluidity of their membranes (Weijers et al., 2007b).

252 Our RDA result shows that MAT and pH have a significant independent effect on
253 the brGDGT distribution in the QTP soils, however, no significant correlation was
254 observed between MAP and brGDGTs ($p > 0.05$; Table 1). Soil pH explaining up to 60.1%
255 of the total variables is the largest contributor to the variance, followed by MAT (up to
256 16.4%) and MAP (up to 10.8%). The predominant influence of soil pH on brGDGT
257 distributions was also observed in global soil dataset (De Jonge et al., 2014; Peterse et
258 al., 2012) and Chinese soils (Yang et al., 2015; Yang et al., 2014). In order to estimate
259 the independent, marginal effect of MAT, MAP and pH, partial RDA (pRDA) was
260 performed. The explained variance of pH still remains high (39.9%), indicating that
261 brGDGT distributions are indeed linked to soil pH, whereas MAT contribute to a smaller
262 amount (10.6%) of the variance (Table 2). Similar to the result of RDA, pRDA also
263 showed minor contribution of MAP (2.0%) to brGDGT distributions. The comparison
264 between RDA and pRDA suggests a decreasing contribution of these three
265 environmental variables (pH, MAT, MAP) when they are considered as a unique
266 contribution (Table 2). Thus, there is a “synergistic effect” (an “antagonistic action”)

267 when MAP and pH (MAT and pH) are considered as covariables, resulting in a positive
268 joint effect of 20.4% for total contribution of pH+MAT+MAP to brGDGT distributions
269 in the QTP soils.

270

271 **3.3 Evaluation of brGDGT-based proxies in the QTP**

272 Since the identification of 6-methyl brGDGTs (De Jonge et al., 2013), a set of new
273 brGDGT indices such as MBT'_{5ME} and CBT_{5ME} have been proposed in order to reduce
274 uncertainty of reconstructed MAT and soil pH (De Jonge et al., 2014; Weijers et al.,
275 2007a; Yang et al., 2015). However, even with application of the MBT_{5ME}-MAT
276 recalibration and the multiple regression, relatively large scatter still exists for those
277 samples from cold regions (De Jonge et al., 2014). Therefore, further calibrations of
278 brGDGT-derived proxies are needed.

279

280 **3.3.1 MAT calibration in cold and dry regions of the QTP**

281 Consistent with the finding of De Jonge et al. (2014), our result shows that CBT_{5ME}
282 no longer contributes significantly to MAT after the exclusion of 6-methyl brGDGTs (p
283 = 0.51; $n = 27$). Therefore, we use MBT'_{5ME} only to calibrate MAT. Considering that
284 limited samples from cold regions were included in previous studies (Peterse et al., 2012;
285 Weijers et al., 2007b), we added our QTP data into the global soil dataset (De Jonge et
286 al., 2014), resulting in a new calibration of MBT'_{5ME}-MAT:

$$287 \text{MAT} = -10.07 + 33.50 \times \text{MBT}'_{5\text{ME}} \\ 288 (n = 249, r^2 = 0.70; \text{RMSE} = 4.7 \text{ }^\circ\text{C}, P < 0.001) \quad (9)$$

289 The correlation coefficient of Eq. 9 ($r^2 = 0.70$) is slightly higher than the previous
290 global calibration ($r^2 = 0.66$; Eq. 4), while its RMSE (4.7 °C) is similar to the previous
291 calibration (4.8 °C; Eq. 4) (De Jonge et al., 2014). Furthermore, the comparison of our
292 estimated MAT and actual MAT ($\Delta\text{MAT} = \text{MAT}_{\text{est}} - \text{MAT}_{\text{act}}$) showed an apparent
293 overestimation (average 2.8 °C; Fig. 5). Therefore, the simple extension of dataset is not
294 successful in improving accuracy of the MBT'_{5ME}-MAT proxy at the global scale.

295 Alternatively, we conducted a regional calibration of MBT'_{5ME} versus MAT based
296 on 27 QTP soils, and a new equation of MBT'_{5ME}-MAT was expressed:

297
$$\text{MAT} = -10.82 + 28.36 \times \text{MBT}'_{5\text{ME}}$$

 298 $(n = 27, r^2 = 0.65; \text{RMSE} = 1.8 \text{ }^\circ\text{C}, P < 0.001)$ (10)

299 The slope of Eq. 10 (28.36) is distinct difference from that of global surface soils
 300 (33.50; Eq. 4). Meanwhile, its RMSE value (1.8 °C) is substantially smaller than that of
 301 De Jonge et al. (2014) (4.8 °C). This reduced uncertainty in reconstructed MAT is
 302 attributed to smaller spatial heterogeneity of soils, similar vegetation types (e.g., alpine
 303 meadow) and a narrower MAT range (-5.5~7.6°C) in the QTP. Usually, the regional
 304 calibration has higher r^2 values than the global one due to its smaller size of dataset and
 305 smaller spatial heterogeneity (Loomis et al., 2014; Yang et al., 2014). However, our
 306 calibration for the QTP has a slightly lower r^2 value (0.65) than the global one (0.70; Eq.
 307 9), suggests that the calibration based on $\text{MBT}'_{5\text{ME}}$ alone is not superior to the traditional
 308 MBT calibration. The RDA result reveals that similar to 5-methyl brGDGTs, 6-methyl
 309 brGDGTs also significantly correlate with MAT (Fig. 4). Thus, we propose a new
 310 brGDGT index ($\text{MBT}_{5/6}$) including 5-methyl brGDGTs used in the traditional definition
 311 and two dominant 6-methyl brGDGTs (IIa' and IIIa'), expressed as:

312
$$\text{MBT}_{5/6} = \frac{\text{Ia} + \text{Ib} + \text{Ic} + \text{IIa}'}{\text{Ia} + \text{Ib} + \text{Ic} + \text{IIa} + \text{IIb} + \text{IIc} + \text{IIIa} + \text{IIIa}'}$$
 (11)

313 Based on data of the QTP soils, the linear correlation of MAT and $\text{MBT}_{5/6}$ was
 314 established as (Fig. 6): $\text{MAT} = -20.14 + 39.51 \times \text{MBT}_{5/6}$

315 $(n = 27, r^2 = 0.82; \text{RMSE} = 1.3 \text{ }^\circ\text{C}, P < 0.001)$ (12)

316 This calibration has substantially higher r^2 (i.e. 0.82) and lower RMSE (i.e. 1.3 °C)
 317 than Eq. 9 (i.e., 0.70 for r^2 and 4.7 °C for RMSE) and Eq. 11 (i.e., 0.65 for r^2 and 1.8 °C
 318 for RMSE), supporting that the inclusion of 5-methyl and 6-methyl brGDGTs is essential
 319 for improved accuracy of MAT reconstruction. However, this result is different from the
 320 finding from the Mount Shennongjia (central China) that 6-methyl brGDGTs are
 321 regarded as the interference, leading to a larger scatter of the MBT' -MAT proxy (Yang
 322 et al., 2015). Nevertheless, these differences highlight the importance of regional
 323 calibrations of brGDGT proxies.

324

325 3.3.2 Effect of soil pH on position of methyl group(s) of brGDGTs

326 It is generally accepted that the proton permeability of the cell membrane plays a
 327 crucial role in maintaining pH gradient across the membrane of bacteria and archaea
 328 (Konings et al., 2002). Weijers et al. (2007b) observed a strong correlation between
 329 relative abundance of cyclopentane moieties of brGDGTs and soil pH, and hypothesized
 330 that, some soil bacteria can change the methyl groups of brGDGTs into cyclopentyl
 331 groups with ambient pH rise, which will loosen the packing of the membrane lipids,
 332 enabling more water molecules to get trapped.

333 Following the approach of De Jonge et al. (2014), we got the following correlation
 334 between soil pH and CBT' which is a modified format of originally defined CBT
 335 (Weijers et al., 2007b):

$$336 \text{ pH} = 7.01 + 1.49 \times \text{CBT}' \quad (n = 27, r^2 = 0.78, \text{RMSE} = 0.30 \text{ pH unit}) \quad (13)$$

337 The Eq. 12 has slightly lower r^2 and substantially lower RMSE compared with the
 338 global calibration of pH-CBT' ($n=221, r^2=0.85, \text{RMSE}=0.52$) (De Jonge et al., 2014),
 339 suggesting that both global and regional calibrations are applicable for soil pH
 340 reconstruction.

341 We noted that some non-cyclopentyl brGDGTs such as Ia, IIa and IIIa show
 342 negative correlations with soil pH, while other brGDGTs show positive correlations with
 343 soil pH in the RDA (Fig. 4). Based on these facts, we put all positively correlated
 344 brGDGTs on the numerator and all negatively correlated brGDGTs on the denominator
 345 to build a new CBT index (or CBT'')

$$346 \text{ CBT}'' = \log \frac{\text{Ib}+\text{Ic}+\text{IIb}+\text{IIc}+\text{IIIb}+\text{IIIc}+\text{IIa}' + \text{IIb}' + \text{IIc}' + \text{IIIa}' + \text{IIIb}' + \text{IIIc}'}{\text{Ia}+\text{IIa}+\text{IIIa}} \quad (14)$$

347 A linear correlation between soil pH and CBT'' was established based on 27 QTP
 348 soils:

$$349 \text{ pH} = 6.93 + 1.49 \times \text{CBT}'' \quad (n = 27, r^2 = 0.80, \text{RMSE} = 0.29 \text{ pH unit}) \quad (15)$$

350 The similar r^2 and RMSE between Eq. 13 and 15 was attributed to minor amounts
 351 of brGDGTs Ib, IIb, IIc, IIIb and IIIc (average 8% of total brGDGTs; Fig. 3) which were
 352 excluded from the CBT' index but included in our CBT'' index.

353 The fractional abundance of 6-methyl brGDGTs showed strong positive
 354 correlations with soil pH in both the QTP ($r^2 = 0.74$; Fig. 8) and global soil dataset (0.41

355 $< r^2 < 0.72$; De Jonge et al., 2014). This is apparent contrast with the previous assumption
 356 that non-cyclopentyl moieties (such as IIa' and IIIa') negatively correlate with soil pH.
 357 Unlike 6-methyl brGDGTs, some 5-methyl brGDGTs did not show positive correlations
 358 with soil pH (de Jonge et al., 2014). Thus, we hypothesize that besides cyclization, the
 359 position of methyl group(s) of brGDGTs also influences cell membrane fluidity. In order
 360 to test this hypothesis, we define a new index about carbon skeleton Isomerism of
 361 Branched Tetraethers (or IBT) as the abundant ratio of non-cyclopentyl 6-methyl to 5-
 362 methyl brGDGTs:

$$363 \text{ IBT} = -\log \frac{\text{IIIa}' + \text{IIa}'}{\text{IIIa} + \text{IIa}} \quad (16)$$

364 We performed a linear regression of IBT versus soil pH based on 27 QTP soils (Fig.
 365 8), yielding an equation as:

$$366 \text{ pH} = 6.77 - 1.56 \times \text{IBT} \quad (\text{n} = 27; r^2 = 0.74, \text{RMSE} = 0.32) \quad (17)$$

367 Meanwhile, the linear correlation of $\text{CBT}_{5\text{ME}}$ and soil pH was also established:

$$368 \text{ pH} = 7.98 - 1.12 \times \text{CBT}_{5\text{ME}} \quad (\text{n} = 27; r^2 = 0.66, \text{RMSE} = 0.37) \quad (18)$$

369 For the regional calibration, the IBT index has higher r^2 and lower RMSE than
 370 traditionally defined $\text{CBT}_{5\text{ME}}$ index, supporting that the carbon skeleton isomerism of
 371 brGDGTs (i.e., changing the position of methyl group) is indeed a physiological
 372 mechanism of brGDGTs-producing bacteria to adapt soil pH change.

373

374 3.3.3 Seasonality of brGDGTs proxies in the QTP

375 The QTP is under strong influence of Asian Monsoon, characterized by
 376 warm/humid summer (June to August) and dry/cold winter (December to February) (An
 377 et al., 2001; Qiu, 2008). In order to examine if there is a seasonal bias on brGDGT
 378 distributions, we analyze the correlation coefficients of 5- and 6-methyl brGDGTs
 379 proxies (i.e., $\text{MBT}'_{5\text{ME}}$, $\text{MBT}_{5/6}$, $\text{CBT}_{5\text{ME}}$ and IBT) versus annual and seasonal air
 380 temperature (Table S2). Overall, there is no apparent seasonal bias for $\text{MBT}'_{5\text{ME}}$ and
 381 $\text{MBT}_{5/6}$. This is likely attributed to significant correlation between seasonal temperature
 382 and MAT in the QTP ($r^2 > 0.80, p < 0.0001$). In addition, no significant correlation was
 383 observed between the CBT indices/IBT and MAT/seasonal temperature ($-0.3 < r < 0.3$;

384 Table S2), suggesting minor influence of air temperature on these indices. Our results
385 are consistent with that of Weijers et al. (2011) who found no significant seasonal bias
386 in MBT-CBT indices in mid-latitude soils. Therefore, the reconstruction of MAT based
387 on the 5- and 6-methyl brGDGTs proxies is doable in the QTP.

388

389 **4. Conclusions**

390 By applying improved chromatography, we successfully separated 5- and 6-methyl
391 brGDGTs in the surface soils from the Qinghai-Tibet Plateau (QTP), a cold and dry
392 region. This is the first time to report 6-methyl brGDGTs in the QTP, providing an
393 opportunity to optimize brGDGTs' proxies in this critical region. Three conclusions were
394 reached based on brGDGT data in 27 surface soils. Firstly, the 6-methyl brGDGTs are
395 widely distributed in the QTP soils accounting for average 53% of total amounts of
396 brGDGTs. Secondly, soil pH is the most important contributor to the variance of
397 brGDGTs, followed by MAT, while MAP has no significant effect on brGDGTs'
398 distributions. Thirdly, two new indices including recently identified 6-methyl brGDGTs
399 were proposed to estimate MAT and soil pH, respectively. The first one, namely MBT_{5/6},
400 is useful for the MAT reconstruction in cold and dry regions (like QTP) with an improved
401 RMSE of 1.3 °C. The second one, namely IBT, is allowed to estimate soil pH with an
402 RMSE of 0.32. Our study demonstrates that besides previously reported cyclization,
403 isomerization of 5-methyl to 6-methyl brGDGTs (expressed as IBT) is another strategy
404 for brGDGTs-producing bacteria to adapt ambient pH change.

405

406 *Acknowledgements.* We are grateful to the National Basic Research Program of China
407 (2014CB954001) and the National Science Foundation of China (41176164; 41476062)
408 for financial support. We also thank Huan Yang for assistance in biomarker analyses.

409

410 **References**

411 An, Z.S., Kutzbach, J.E., Prell, W.L., Porter, S.C., Evolution of Asian monsoons and
412 phased uplift of the Himalayan Tibetan plateau since Late Miocene times. *Nature*,
413 411, 62-66, 2001.

414 Ballantyne, A.P., Greenwood, D.R., Sinninghe Damsté, J.S., Csank, A.Z., Eberle, J.J.,
415 Rybczynski, N., Significantly warmer Arctic surface temperatures during the
416 Pliocene indicated by multiple independent proxies. *Geology*, 38, 603-606, 2010.

417 Bendle, J.A., Weijers, J.W.H., Maslin, M.A., Damste, J.S.S., Schouten, S., Hopmans,
418 E.C., Boot, C.S., Pancost, R.D., Major changes in glacial and Holocene terrestrial
419 temperatures and sources of organic carbon recorded in the Amazon fan by
420 tetraether lipids. *Geochem. Geophys. Geosy.*, 11, doi: 10.1029/2010gc003308,
421 2010.

422 Blaga, C.I., Reichart, G.-J., Heiri, O., Damste, J.S.S., Tetraether membrane lipid
423 distributions in water-column particulate matter and sediments: a study of 47
424 European lakes along a north-south transect. *J. Paleolimnol.*, 41, 523-540, 2009.

425 Blaga, C.I., Reichart, G.-J., Schouten, S., Lotter, A.F., Werne, J.P., Kosten, S., Mazzeo,
426 N., Lacerot, G., Sinninghe Damsté, J.S., Branched glycerol dialkyl glycerol
427 tetraethers in lake sediments: Can they be used as temperature and pH proxies?
428 *Org. Geochem.*, 41, 1225-1234, 2010.

429 Brassell, S.C., Eglinton, G., Marlowe, I.T., Pflaumann, U., Sarnthein, M., Molecular
430 stratigraphy: a new tool for climatic assessment. *Nature*, 320, 129-133, 1986.

431 Cheng, W., Zhao, S., Zhou, C., Chen, X., Simulation of the Decadal Permafrost
432 Distribution on the Qinghai-Tibet Plateau (China) over the Past 50 Years.
433 *Permafrost and Periglacial Processes*, 23, 292-300, 2012.

434 Chu, G.Q., Sun, Q., Li, S.Q., Zheng, M.P., Jia, X.X., Lu, C.F., Liu, J.Q., Liu, T.S., Long-
435 chain alkenone distributions and temperature dependence in lacustrine surface
436 sediments from China. *Geochim. Cosmochim. Acta*, 69, 4985-5003, 2005.

437 D'Anjou, R.M., Wei, J.H., Castaneda, I.S., Brigham-Grette, J., Petsch, S.T., Finkelstein,
438 D.B., High-latitude environmental change during MIS 9 and 11: biogeochemical
439 evidence from Lake El'gygytgyn, Far East Russia. *Clim. Past.*, 9, 567-581, 2013.

440 De Jonge, C., Hopmans, E.C., Stadnitskaia, A., Rijpstra, W.I.C., Hofland, R., Tegelaar,
441 E., Sinninghe Damsté, J.S., Identification of novel penta- and hexamethylated
442 branched glycerol dialkyl glycerol tetraethers in peat using HPLC-MS2, GC-
443 MS and GC-SMB-MS. *Org. Geochem.*, 54, 78-82, 2013.

- 444 De Jonge, C., Hopmans, E.C., Zell, C.I., Kim, J.-H., Schouten, S., Sinninghe Damsté,
445 J.S., Occurrence and abundance of 6-methyl branched glycerol dialkyl glycerol
446 tetraethers in soils: Implications for palaeoclimate reconstruction. *Geochim.*
447 *Cosmochim. Acta*, 141, 97-112, 2014.
- 448 Dirghangi, S.S., Pagani, M., Hren, M.T., Tipple, B.J., Distribution of glycerol dialkyl
449 glycerol tetraethers in soils from two environmental transects in the USA. *Org.*
450 *Geochem.*, 59, 49-60, 2013.
- 451 Fietz, S., Huguet, C., Bendle, J., Escala, M., Gallacher, C., Herfort, L., Jamieson, R.,
452 Martinez-Garcia, A., McClymont, E.L., Peck, V.L., Prahl, F.G., Rossi, S., Rueda,
453 G., Sanson-Barrera, A., Rosell-Mele, A., Co-variation of crenarchaeol and
454 branched GDGTs in globally-distributed marine and freshwater sedimentary
455 archives. *Glob. Planet. Change*, 92-93, 275-285, 2012.
- 456 Günther, F., Thiele, A., Gleixner, G., Xu, B., Yao, T., Schouten, S., Distribution of
457 bacterial and archaeal ether lipids in soils and surface sediments of Tibetan lakes:
458 Implications for GDGT-based proxies in saline high mountain lakes. *Org.*
459 *Geochem.*, 67, 19-30, 2014.
- 460 He, L., Zhang, C.L., Dong, H., Fang, B., Wang, G., Distribution of glycerol dialkyl
461 glycerol tetraethers in Tibetan hot springs. *Geosci. Front.*, 3, 289-300, 2012.
- 462 Hijmans, R.J., Cameron, S.E., Parra, J.L., Jones, P.G., Jarvis, A., Very high resolution
463 interpolated climate surfaces for global land areas. *Int. J. Climatol.*, 25, 1965-
464 1978, 2005.
- 465 Huguet, C., Hopmans, E.C., Febo-Ayala, W., Thompson, D.H., Sinninghe Damsté, J.S.,
466 Schouten, S., An improved method to determine the absolute abundance of
467 glycerol dibiphytanyl glycerol tetraether lipids. *Org. Geochem.*, 37, 1036-1041,
468 2006.
- 469 Kang, S., Xu, Y., You, Q., Fluegel, W.-A., Pepin, N., Yao, T., Review of climate and
470 cryospheric change in the Tibetan Plateau. *Environ. Res. Lett.*, 5, 2010.
- 471 Keatley, B., Douglas, M.V., Blais, J., Mallory, M., Smol, J., Impacts of seabird-derived
472 nutrients on water quality and diatom assemblages from Cape Vera, Devon Island,
473 Canadian High Arctic. *Hydrobiologia*, 621, 191-205, 2009.

- 474 Konings, W., Albers, S.-V., Koning, S., Driessen, A.M., The cell membrane plays a
475 crucial role in survival of bacteria and archaea in extreme environments. *Antonie*
476 *Van Leeuwenhoek*, 81, 61-72, 2002.
- 477 Li, J.J., The environmental effects of the uplift of the Qinghai-Xizang Plateau. *Quat. Sci.*
478 *Rev.*, 10, 479-483, 1991.
- 479 Lin, X., Zhu, L., Wang, Y., Wang, J., Xie, M., Ju, J., Mäusbacher, R., Schwalb, A.,
480 Environmental changes reflected by n-alkanes of lake core in Nam Co on the
481 Tibetan Plateau since 8.4 kaB.P. *Chin. Sci. Bull.*, 53, 3051-3057, 2008.
- 482 Liu, W., Liu, Z., Wang, H., He, Y., Wang, Z., Xu, L., Salinity control on long-chain
483 alkenone distributions in lake surface waters and sediments of the northern
484 Qinghai-Tibetan Plateau, China. *Geochim. Cosmochim. Acta*, 75, 1693-1703,
485 2011.
- 486 Liu, W., Wang, H., Zhang, C.L., Liu, Z., He, Y., Distribution of glycerol dialkyl glycerol
487 tetraether lipids along an altitudinal transect on Mt. Xiangpi, NE Qinghai-Tibetan
488 Plateau, China. *Org. Geochem.*, 57, 76-83, 2013.
- 489 Liu, X.D., Chen, B.D., Climatic warming in the Tibetan Plateau during recent decades.
490 *Int. J. Climatol.*, 20, 1729-1742, 2000.
- 491 Liu, Z., Henderson, A.C.G., Huang, Y., Alkenone-based reconstruction of late-Holocene
492 surface temperature and salinity changes in Lake Qinghai, China. *Geophys. Res.*
493 *Lett.*, 33, 2006.
- 494 Loomis, S.E., Russell, J.M., Eggermont, H., Verschuren, D., Sinninghe Damsté, J.S.,
495 Effects of temperature, pH and nutrient concentration on branched GDGT
496 distributions in East African lakes: Implications for paleoenvironmental
497 reconstruction. *Org. Geochem.*, 66, 25-37, 2014.
- 498 Loomis, S.E., Russell, J.M., Ladd, B., Street-Perrott, F.A., Sinninghe Damsté, J.S.,
499 Calibration and application of the branched GDGT temperature proxy on East
500 African lake sediments. *Earth Planet. Sci. Lett.*, 357-358, 277-288, 2012.
- 501 Menges, J., Huguet, C., Alcañiz, J.M., Fietz, S., Sachse, D., Rosell-Melé, A., Influence
502 of water availability in the distributions of branched glycerol dialkyl glycerol
503 tetraether in soils of the Iberian Peninsula. *Biogeosciences*, 11, 2571-2581, 2014.

- 504 Meriläinen, J., Hynynen, J., Palomäki, A., Reinikainen, P., Teppo, A., Granberg, K.,
505 Importance of diffuse nutrient loading and lake level changes to the
506 eutrophication of an originally oligotrophic boreal lake: a palaeolimnological
507 diatom and chironomid analysis. *J. Paleolimnol.*, 24, 251-270, 2000.
- 508 Pearson, E.J., Juggins, S., Talbot, H.M., Weckström, J., Rosén, P., Ryves, D.B., Roberts,
509 S.J., Schmidt, R., A lacustrine GDGT-temperature calibration from the
510 Scandinavian Arctic to Antarctic: Renewed potential for the application of
511 GDGT-paleothermometry in lakes. *Geochim. Cosmochim. Acta*, 75, 6225-6238,
512 2011.
- 513 Peterse, F., Prins, M.A., Beets, C.J., Troelstra, S.R., Zheng, H., Gu, Z., Schouten, S.,
514 Damsté, J.S.S., Decoupled warming and monsoon precipitation in East Asia over
515 the last deglaciation. *Earth Planet. Sci. Lett.*, 301, 256-264, 2011.
- 516 Peterse, F., van der Meer, J., Schouten, S., Weijers, J.W.H., Fierer, N., Jackson, R.B.,
517 Kim, J.-H., Sinninghe Damsté, J.S., Revised calibration of the MBT-CBT
518 paleotemperature proxy based on branched tetraether membrane lipids in surface
519 soils. *Geochim. Cosmochim. Acta*, 96, 215-229, 2012.
- 520 Prahl, F.G., Muehlhausen, L.A., Zahnle, D.L., Further evaluation of long-chain
521 alkenones as indicators of paleoceanographic conditions. *Geochim. Cosmochim.*
522 *Acta*, 52, 2303-2310, 1988.
- 523 Qiu, J., The third pole. *Nature*, 454, 393-396, 2008.
- 524 Schouten, S., Hopmans, E.C., Sinninghe Damsté, J.S., The organic geochemistry of
525 glycerol dialkyl glycerol tetraether lipids: A review. *Org. Geochem.*, 54, 19-61,
526 2013.
- 527 Seppä, H., Birks, H.J.B., July mean temperature and annual precipitation trends during
528 the Holocene in the Fennoscandian tree-line area: pollen-based climate
529 reconstructions. *The Holocene*, 11, 527-539, 2001.
- 530 Shanahan, T.M., Hughen, K.A., Van Mooy, B.A.S., Temperature sensitivity of branched
531 and isoprenoid GDGTs in Arctic lakes. *Org. Geochem.*, 64, 119-128, 2013.
- 532 Sinninghe Damsté, J.S., Ossebaar, J., Abbas, B., Schouten, S., Verschuren, D., Fluxes
533 and distribution of tetraether lipids in an equatorial African lake: Constraints on

534 the application of the TEX86 palaeothermometer and BIT index in lacustrine
535 settings. *Geochim. Cosmochim. Acta*, 73, 4232-4249, 2009.

536 Sinninghe Damsté, J.S., Rijpstra, W.I.C., Hopmans, E.C., Weijers, J.W.H., Foesel, B.U.,
537 Overmann, J., Dedysh, S.N., 13,16-Dimethyl Octacosanedioic Acid (iso-
538 Diabolic Acid), a Common Membrane-Spanning Lipid of Acidobacteria
539 Subdivisions 1 and 3. *Appl. Environ. Microbiol.*, 77, 4147-4154, 2011.

540 Sun, Q., Chu, G., Liu, M., Xie, M., Li, S., Ling, Y., Wang, X., Shi, L., Jia, G., Lü, H.,
541 Distributions and temperature dependence of branched glycerol dialkyl glycerol
542 tetraethers in recent lacustrine sediments from China and Nepal. *J. Geophys.*
543 *Res.-Biogeo.*, 116, G01008, doi: 10.1029/2010jg001365, 2011.

544 Thompson, L.G., Yao, T., Davis, M.E., Henderson, K.A., MosleyThompson, E., Lin,
545 P.N., Beer, J., Synal, H.A., ColeDai, J., Bolzan, J.F., Tropical climate instability:
546 The last glacial cycle from a Qinghai-Tibetan ice core. *Science*, 276, 1821-1825,
547 1997.

548 Tierney, J.E., Russell, J.M., Distributions of branched GDGTs in a tropical lake system:
549 Implications for lacustrine application of the MBT/CBT paleoproxy. *Org.*
550 *Geochem.*, 40, 1032-1036, 2009.

551 van den Wollenberg, A., Redundancy analysis an alternative for canonical correlation
552 analysis. *Psychometrika*, 42, 207-219, 1977.

553 Wang, H., Liu, W., Zhang, C.L., Wang, Z., Wang, J., Liu, Z., Dong, H., Distribution of
554 glycerol dialkyl glycerol tetraethers in surface sediments of Lake Qinghai and
555 surrounding soil. *Org. Geochem.*, 47, 78-87, 2012.

556 Wang, Y., Kromhout, E., Zhang, C., Xu, Y., Parker, W., Deng, T., Qiu, Z., Stable isotopic
557 variations in modern herbivore tooth enamel, plants and water on the Tibetan
558 Plateau: Implications for paleoclimate and paleoelevation reconstructions.
559 *Palaeogeogr. Palaeoclimatol. Palaeoecol.*, 260, 359-374, 2008.

560 Weijers, J.W.H., Bernhardt, B., Peterse, F., Werne, J.P., Dungait, J.A.J., Schouten, S.,
561 Sinninghe Damsté, J.S., Absence of seasonal patterns in MBT–CBT indices in
562 mid-latitude soils. *Geochim. Cosmochim. Acta*, 75, 3179-3190, 2011.

563 Weijers, J.W.H., Schefuss, E., Schouten, S., Damste, J.S.S., Coupled thermal and

- 564 hydrological evolution of tropical Africa over the last deglaciation. *Science*, 315,
565 1701-1704, 2007a.
- 566 Weijers, J.W.H., Schouten, S., Spaargaren, O.C., Sinninghe Damsté, J.S., Occurrence
567 and distribution of tetraether membrane lipids in soils: Implications for the use
568 of the TEX86 proxy and the BIT index. *Org. Geochem.*, 37, 1680-1693, 2006.
- 569 Weijers, J.W.H., Schouten, S., van den Donker, J.C., Hopmans, E.C., Sinninghe Damsté,
570 J.S., Environmental controls on bacterial tetraether membrane lipid distribution
571 in soils. *Geochim. Cosmochim. Acta*, 71, 703-713, 2007b.
- 572 Wu, W., Ruan, J., Ding, S., Zhao, L., Xu, Y., Yang, H., Ding, W., Pei, Y., Source and
573 distribution of glycerol dialkyl glycerol tetraethers along lower Yellow River-
574 estuary-coast transect. *Mar. Chem.*, 158, 17-26, 2014.
- 575 Wu, X., Dong, H., Zhang, C.L., Liu, X., Hou, W., Zhang, J., Jiang, H., Evaluation of
576 glycerol dialkyl glycerol tetraether proxies for reconstruction of the paleo-
577 environment on the Qinghai-Tibetan Plateau. *Org. Geochem.*, 61, 45-56, 2013.
- 578 Xie, S., Pancost, R.D., Chen, L., Evershed, R.P., Yang, H., Zhang, K., Huang, J., Xu, Y.,
579 Microbial lipid records of highly alkaline deposits and enhanced aridity
580 associated with significant uplift of the Tibetan Plateau in the Late Miocene.
581 *Geology*, 40, 291-294, 2012.
- 582 Yang, H., Lü, X., Ding, W., Lei, Y., Dang, X., Xie, S., The 6-methyl branched tetraethers
583 significantly affect the performance of the methylation index (MBT') in soils
584 from an altitudinal transect at Mount Shennongjia. *Org. Geochem.*, 82, 42-53,
585 2015.
- 586 Yang, H., Pancost, R.D., Dang, X., Zhou, X., Evershed, R.P., Xiao, G., Tang, C., Gao,
587 L., Guo, Z., Xie, S., Correlations between microbial tetraether lipids and
588 environmental variables in Chinese soils: Optimizing the paleo-reconstructions
589 in semi-arid and arid regions. *Geochim. Cosmochim. Acta*, 126, 49-69, 2014.
- 590 Yao, T., Pu, J., Lu, A., Wang, Y., Yu, W., Recent Glacial Retreat and Its Impact on
591 Hydrological Processes on the Tibetan Plateau, China, and Surrounding Regions.
592 *Arct. Antarct. Alp. Res.*, 39, 642-650, 2007.
- 593 Yao, T.D., Thompson, L.G., Duan, K.Q., Xu, B.Q., Wang, N.L., Pu, J.C., Tian, L.D., Sun,

594 W.Z., Kang, S.C., Qin, X.A., Temperature and methane records over the last 2 ka
595 in Dasuopu ice core. *Sci. China Ser. D*, 45, 1068-1074, 2002.

596 Zech, R., Gao, L., Tarozo, R., Huang, Y., Branched glycerol dialkyl glycerol tetraethers
597 in Pleistocene loess-paleosol sequences: Three case studies. *Org. Geochem.*, 53,
598 38-44, 2012.

599 Zell, C., Kim, J.-H., Hollander, D., Lorenzoni, L., Baker, P., Silva, C.G., Nittrouer, C.,
600 Sinninghe Damsté, J.S., Sources and distributions of branched and isoprenoid
601 tetraether lipids on the Amazon shelf and fan: Implications for the use of GDGT-
602 based proxies in marine sediments. *Geochim. Cosmochim. Acta*, 139, 293-312,
603 2014.

604 Zink, K.-G., Vandergoes, M.J., Mangelsdorf, K., Dieffenbacher-Krall, A.C., Schwark,
605 L., Application of bacterial glycerol dialkyl glycerol tetraethers (GDGTs) to
606 develop modern and past temperature estimates from New Zealand lakes. *Org.*
607 *Geochem.*, 41, 1060-1066, 2010.

608 Zink, K.G., Leythaeuser, D., Melkonian, M., Schwark, L., Temperature dependency of
609 long-chain alkenone distributions in Recent to fossil limnic sediments and in lake
610 waters. *Geochim. Cosmochim. Acta*, 65, 253-265, 2001.

611

612

613

614

615

616

617

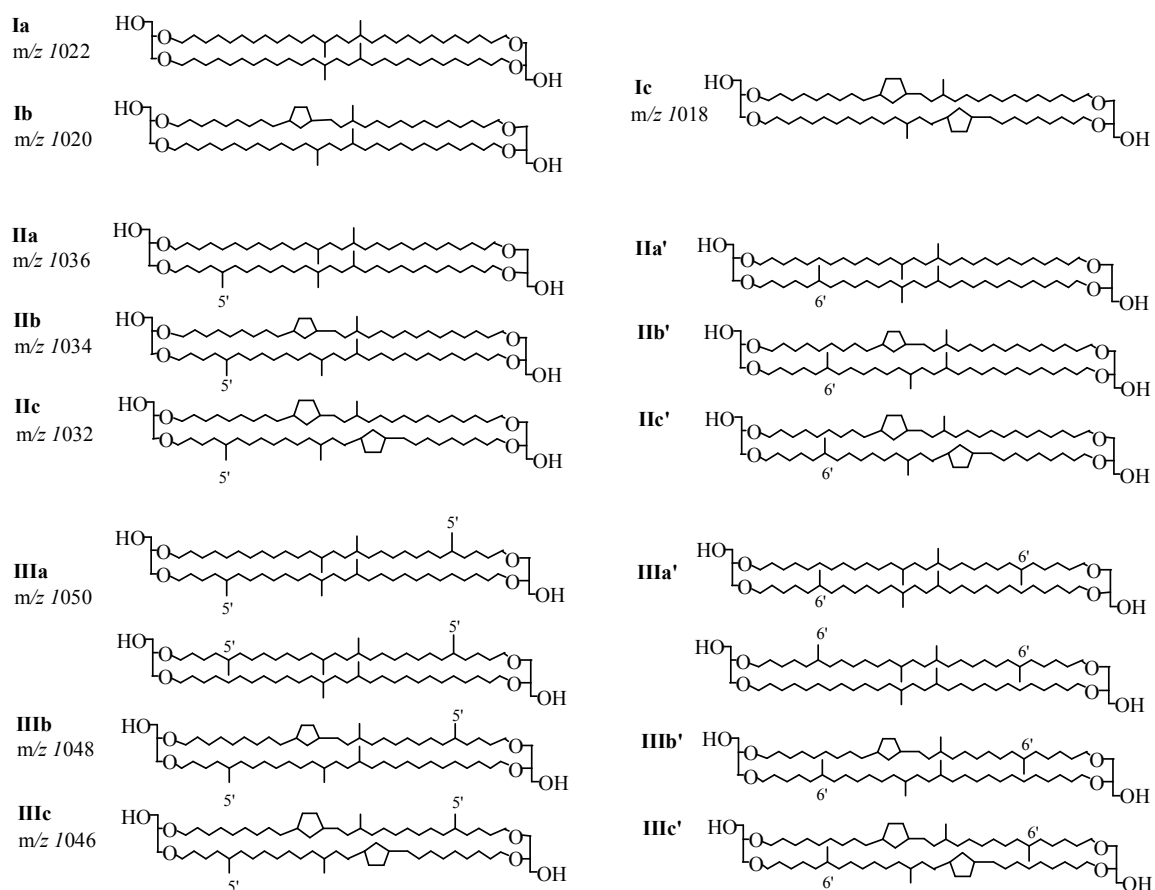
618

619

620

621

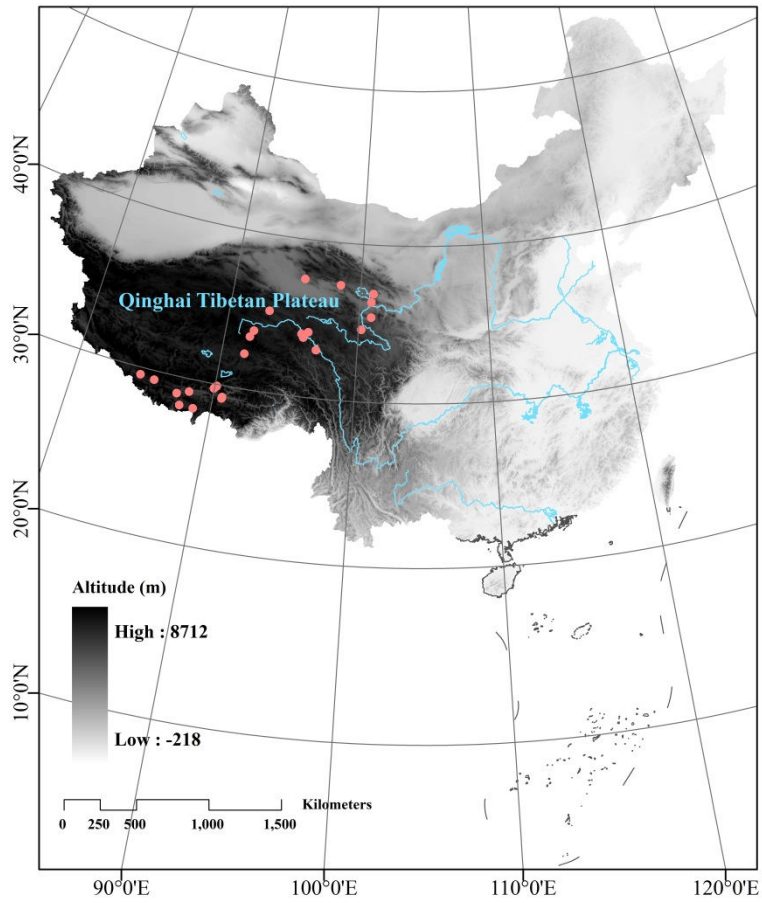
622



623

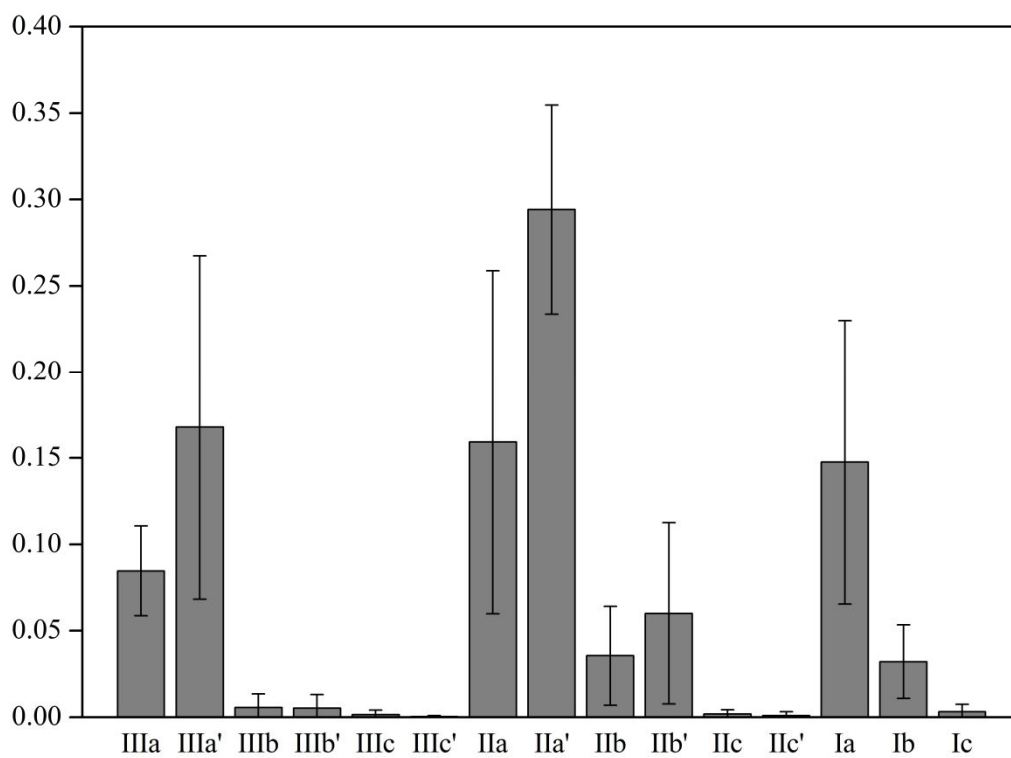
624 **Fig. 1.** Molecular structures of 5- and 6-methyl branched GDGTs used in this study. The
 625 compounds that have one or two methyl groups at the $\alpha 6$ or $\omega 6$ position are defined as
 626 6-methyl brGDGTs, while the compounds that have one or two methyl groups at the $\alpha 5$
 627 or $\omega 5$ position are defined as 5-methyl brGDGTs.

628



629
630
631
632
633
634
635
636

Fig. 2. Locations of soil sampling sites (n = 30) in the QTP (Pink solid circles).



637

638 **Fig. 3.** Average ($n = 27$) fractional abundance of brGDGTs in surface soils of the QTP.

639

640

641

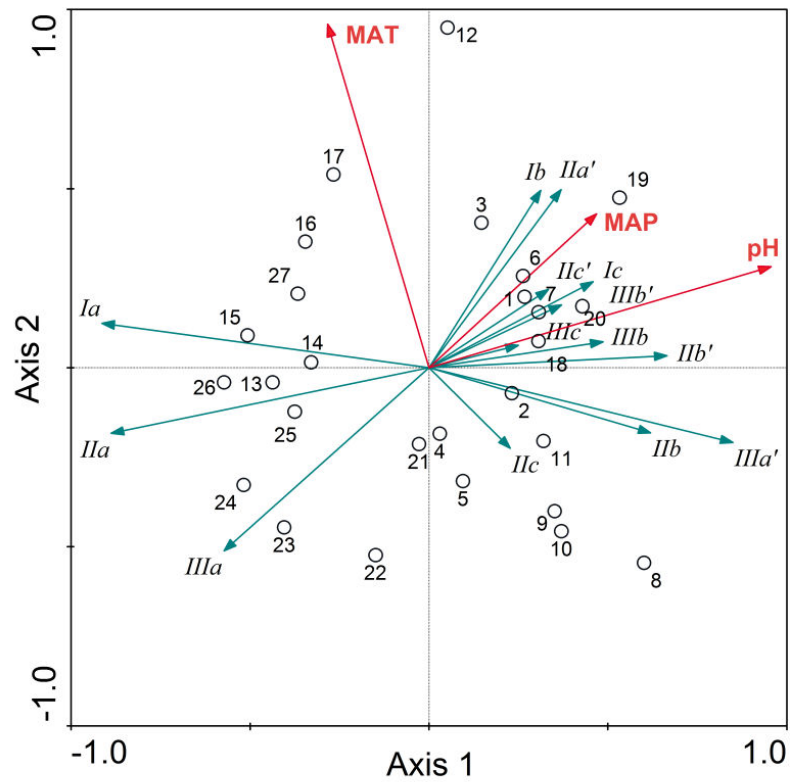
642

643

644

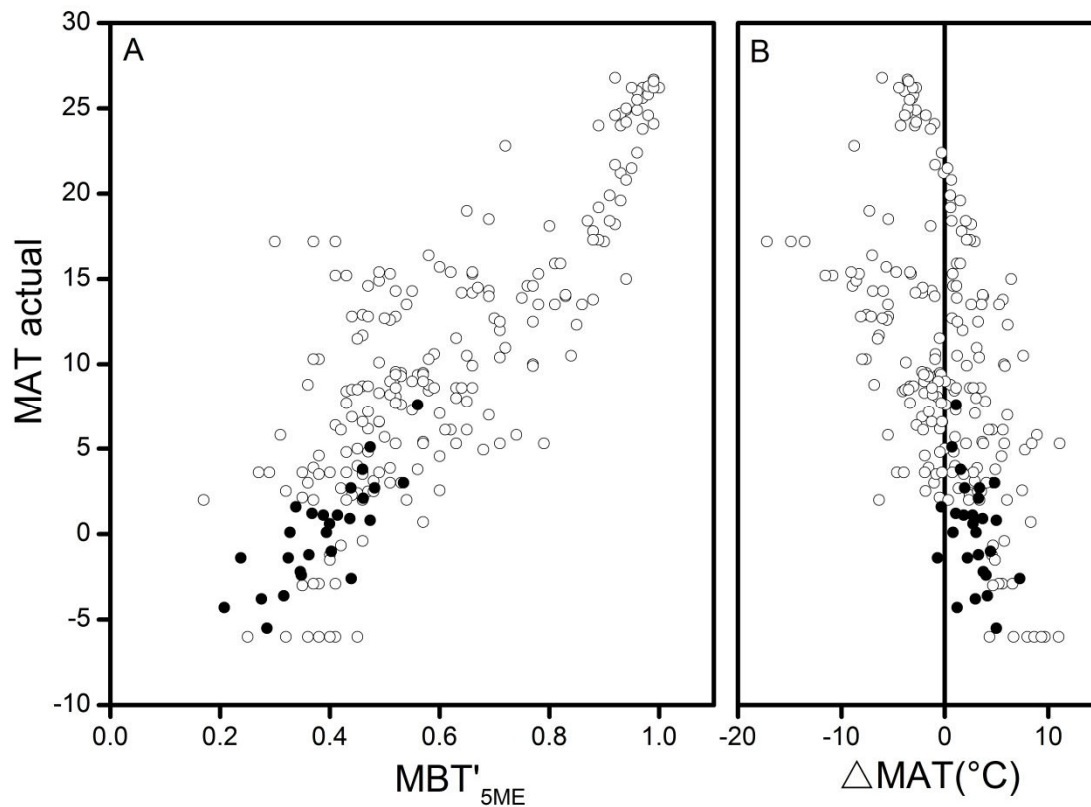
645

646



647
 648 **Fig. 4.** RDA triplot showing the relationship between 5- and 6-methyl brGDGTs%, MAT,
 649 MAP and soil pH from the QTP. Numbers in the plot correspond to the soils in
 650 supplementary material (Table S1). The first and second axis explained 65.2% and 6.1%
 651 of the variance, respectively.

652
 653
 654
 655
 656



657

658 **Fig. 5.** A) Scatterplot of MBT'5ME with actual MAT; B: difference between estimated
 659 MAT and actual MAT (Δ MAT). Solid and empty circles represented soils in this study
 660 and global soils (de Jonge et al., 2014), respectively.

661

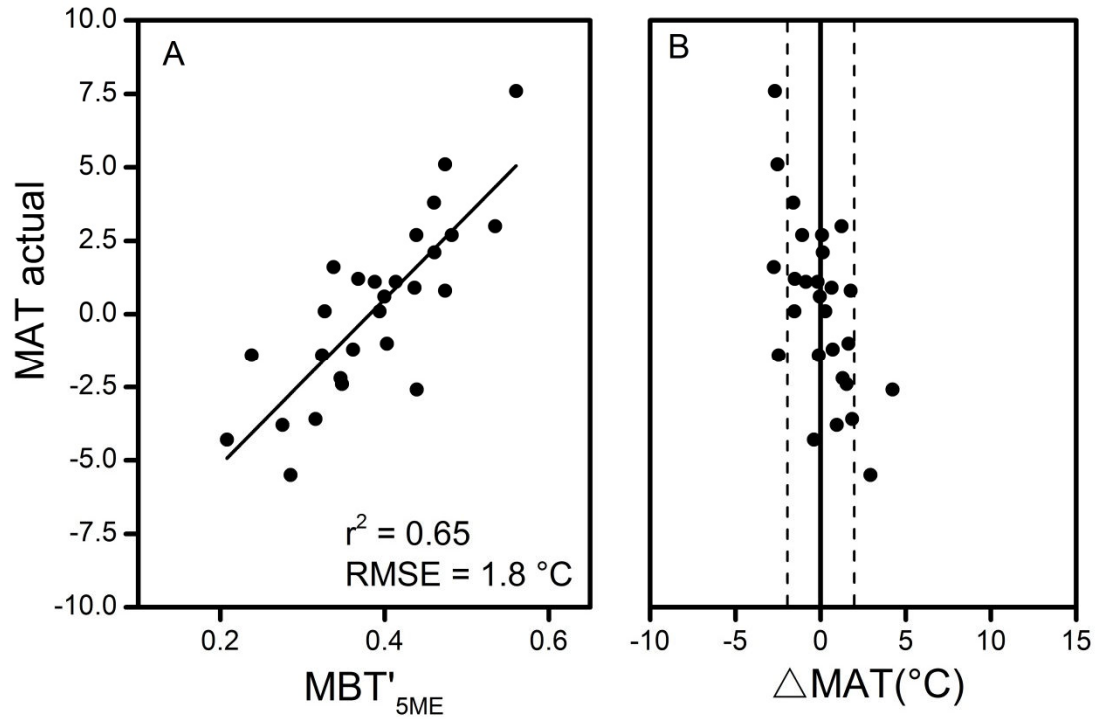
662

663

664

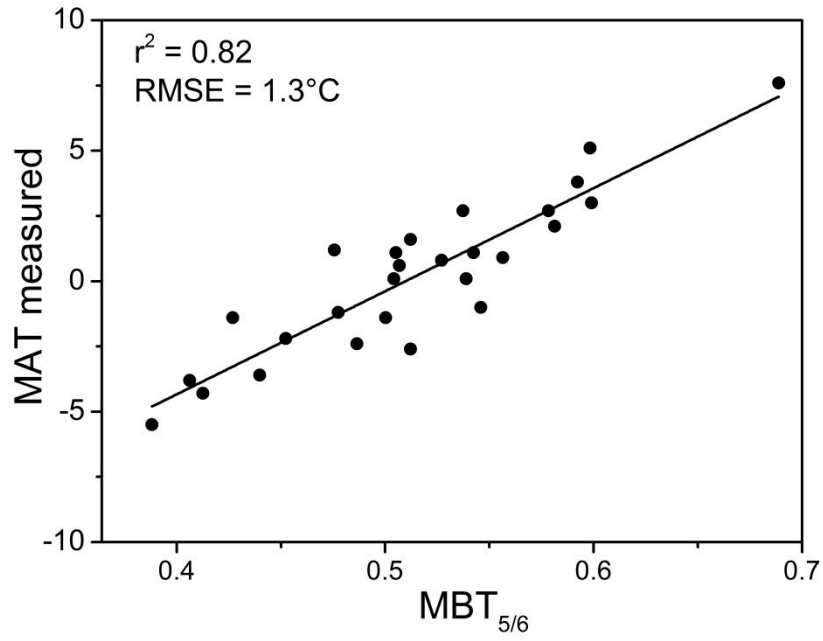
665

666



667
 668 **Fig. 6.** A) Linear regression of MBT'_{5ME} with actual MAT; B) difference between
 669 estimated MAT and actual MAT (ΔMAT). Data are from this study for 27 surface soils
 670 of the QTP.

671
 672
 673
 674
 675
 676
 677
 678
 679
 680
 681
 682



683

684 **Fig. 7.** Linear regression plot of MBT_{5/6} versus MAT in the QTP.

685

686

687

688

689

690

691

692

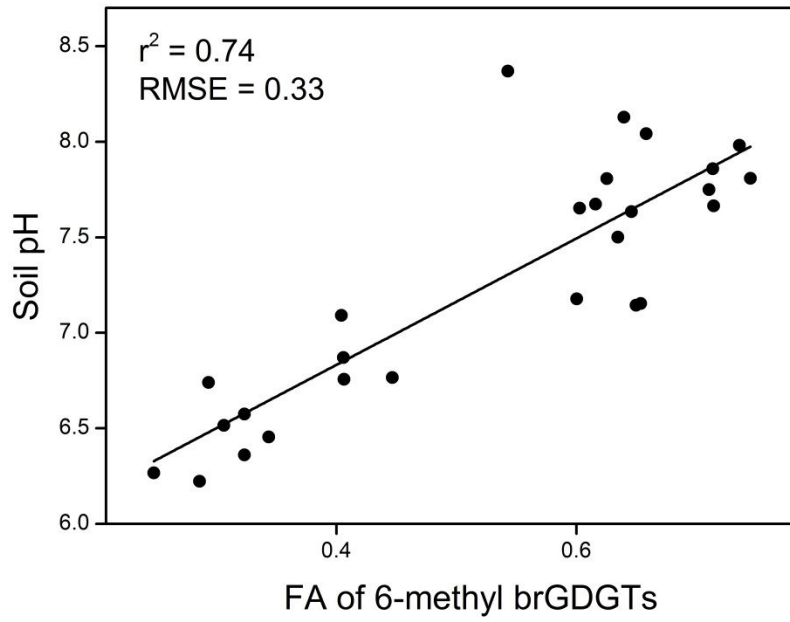
693

694

695

696

697



698

699 **Fig. 8.** Plots of fractional abundance of 6-methyl brGDGTs of the total amount of
 700 brGDGTs (f_{6ME}) versus soil pH in the QTP.

701

702

703

704

705

706

707

708

709

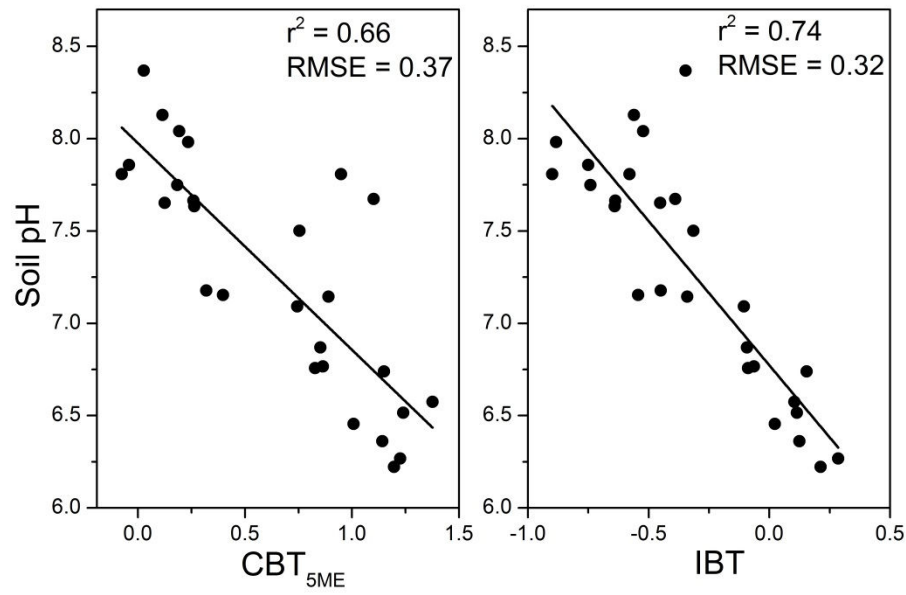
710

711

712

713

714



715

716 **Fig. 9.** Scatterplots of A) soil pH versus CBT_{5ME} and B) soil pH versus IBT based on 27

717 soil samples in the QTP.

718

719

720

721

722

723

724

725

726

727

728

729

730

731

732

733

734

735

736 **Table 1:** Results of RDA and partial RDA (pRDA) showing the total and unique
 737 contributions of soil pH, MAT and MAP to the variance in brGDGT distributions in the
 738 QTP soils.

Variables	Total contribution (%)		Unique contribution (%)	
	<i>p</i> Value	Max eigenvalues*	<i>p</i> Value	Eigenvalues
pH	0.001	60.1	0.001	39.9
MAT	0.001	16.4	0.001	10.6
MAP	0.179	10.8	0.172	2.0
All variables	0.001	72.9		
Joint effects				20.4
MAT + pH	0.001	56.4		
MAT + MAP	0.001	12.8		
MAP + pH	0.001	62.1		

739 *The first environmental variable which has been selected into the analysis has the maximum eigenvalues (explained
 740 variances), there are 6 sequences with different arrangement of pH, MAT and MAP. However, no matter which
 741 sequence has been selected for RDA, the total variables contribution is invariant.

742

743